Electronic Supplementary Material (ESI) for ChemComm.

Supporting information

Synergistic Phototherapy of NIR Wavelength Xanthene-quinoline Salt-Based Heavy Atoms-free Phtosensitizers for Tumor Therapy

Long He[II], Lin-Hui He[II], Huan-Hua Lai, Shuai Xu*, Jiao-Liang Wang, Jun-Chao Xu, Ling Shi*, Lin Yuan

Table of contents:

1. **Experimental details**.....- 2 -
2. **Compound Synthesis**.....- 5 -
3. **Supplemental Table and Figures**.....- 7 -
4. **NMR and Mass Spectra**.....- 18 -
5. **References**.....- 25 -

1. Experimental details

Materials and instruments. Unless otherwise stated, all reagents were purchased from commercial suppliers and used without further purification. Solvents were purified by standard methods prior to use. High resolution mass spectra were performed using a Bruker Daltonics micro-TOF-Q II mass spectrometer. High resolution mass spectra were performed using a Bruker Daltonics micro-TOF-Q II mass spectrometer. NMR spectra were recorded on Bruker-400, using TMS as the internal standard. Absorption spectra were recorded on a UV-3600 spectrophotometer (Shimadzu Corporation, Japan). Photoluminescence spectra were recorded on HITACHI F7000 fluorescence spectrometer with a 1 cm standard quartz cell. Fluorescence imaging of fluorescently stained cells were performed on a confocal laser scanning microscope (CLSM, C1-Si, Nikon, Japan) or inverted microscope (Zeiss Axio Observer, Germany). The in vivo (living mice) imaging was carried out using an IVIS Lumina XR (IS1241N6071) in vivo imaging system. The pH measurements were carried out on a Mettler-Toledo Delta 320 pH meter. TLC analysis was performed on silica gel plates and column chromatography was conducted over silica gel (mesh 200–300) columns, obtained from the Yantai Jiangyou silica gel Development Company Limited.

Calculation of fluorescence quantum yield. Fluorescence quantum yield was determined using optically matching solutions of ICG (Φ_f = 13% in eathol at 25 °C)[1] as the standard and the quantum yield was calculated using the following equation:

$$\Phi_s = \Phi_r(A_r F_s / A_s F_r)\,(n_s^2/n_r^2)$$

where, s and r denote sample and reference, respectively. *A* is the absorbance. *F* is the relative integrated fluorescence intensity and n is the refractive index of the solvent.

DFT calculations. All the geometrical optimizations and TDDFT calculations for vertical excitation were performed using B3LYP functional and the 6-31G*(d) basis set for H, C, N, O atoms. The molecular orbital information including energy levels and distribution was obtained at the same theoretical level. The above calculations were carried out in Gaussian 09 program package.[2]

Reactive oxygen species (ROS) generation measurement in vitro. The general ROS generation measurements were conducted using 1,3-Diphenylisobenzofuran (DPBF 50 μM) as the indicator in methanol solution, the absorption signal of indicator was monitored at 410 nm with the 808 nm laser irradiation of 250 mW/cm^2 in the presence/absence of **CSQs**. The $^1O_2$ generation measurements were conducted using Singlet Oxygen Sensor Green (SOSG, 10 μM) in methanol system, the fluorescence signal of indicator was monitored in a range of 500-750 nm with a 480 nm excitation under 808 nm laser irradiation of 250 mW/cm^2 in the presence/absence of **CSQ-Ph**.

Singlet oxygen yield (Φ_Δ) was calculated using optically matching solutions of ICG ($\Phi_{\Delta std}$ = 0.16 in methanol at 25 °C) as the standard[3] and the Φ_Δ was calculated using the

following:[4]

$$\Phi_{\Delta sam} = \Phi_{\Delta std}(m_{sam}/m_{std})(F_{std}/F_{sam})$$

Where “sam” and “std” represent the “PSs” and “ICG”, respectively. “m” is the slope of absorbance change curve of DPBF at 415 nm, $F=1-10^{-O.D.}$ (O.D. is the absorbance of the solution at 808 nm).

ROS generation measurement in cell. The general ROS generation measurements were conducted using 2,7-dichlorodihydrofluorescein diacetate (DCFH-DA) as the indicator. HeLa cells were grown in imaging dish at 37°C for 24 h. they were divided into four groups: control group, irradiation group, **CSQ-Ph** (5 μM) non-radiation group and **CSQ-Ph** (5 μM) irradiation group. Cells were exposed to 808 nm laser (375 mW/cm^2) irradiation for 1 min. Then, stained with medium containing DCFH-DA (10 μM) for 30 min, the cells were imaged using CLSM. For DCFH-DA, the excitation was 488 nm, and the emission filter was 500–550 nm.

Photothermal effect and photothermal conversion efficiency. The solutions of **CSQs** (at the concentrations of 0, 10, 25, and 50 μM) in glass vials were irradiated by 808 nm laser (250 mW/cm^2) for 5 min, and 50 μM **CSQs** (at the power density of 125, 250 and 375 mW/cm^2) in glass vials were irradiated by 808 nm laser for 5 min, respectively. Meanwhile, the temperatures of solutions were recorded using a thermal imager. To assess the photothermal conversion efficiency, the solutions of free **CSQs** in glass vials were irradiated by 808 nm laser (250 mW/cm^2) for 5 min, when the temperature reached a plateau, the irradiation was removed for cooling down to room temperature. The temperature of the solutions was recorded for 10 min, and then their photothermal conversion efficiencies were calculated according to reported method.[4]

Cell culture. HeLa cells, A549 cells and 4T1 Cells were cultured in high glucose Dulbecco's Modified Eagle Medium (DMEM, Hyclone) supplemented with 10% fetal bovine serum (FBS, BI), and 1% antibiotics (100 U/mL penicillin and 100 μg/mL streptomycin, Hyclone) at 37°C and 5% CO_2. Cells were carefully harvested and split when they reached 80% confluence to maintain exponential growth.

Cytotoxicity of CSQs. HeLa cells were cultured at 37°C in a 5% CO_2/95% air in a 96-well plate at a density of 1×10^4 cells for 24 hours. Then, the DMEM medium was replaced by different concentrations of **CSQs** (0-20 μM) for further incubation with cells for 24 h. Finally, the cell viability was assessed by standard MTT assay.

Live-dead cell staining. HeLa cells were grown in four-hole dish at 37°C for 24 h. they were divided into four groups: control group, irradiation group, **CSQ-Ph** (10 μM) non-radiation group and **CSQ-Ph** (10 μM) irradiation group. Cells were exposed to 808 nm laser (375 mW/cm^2) irradiation for 5 min. Then, stained with medium containing calcein AM (2 μM) and PI (2 μM) for 30 min, the cells were imaged using inverted microscope. For calcein AM, the excitation was 488 nm, and the emission filter was 500–550 nm; For PI, the excitation was 560 nm, and the emission filter was 570-630 nm.

4T1-induced tumor. All animal procedures were performed in accordance with protocol No. SYXK (Xiang) 2018-0006 approved by the Laboratory Animal Center of Hunan and experiments were approved by the Animal Ethics Committee of College of Biology (Hunan University). Subcutaneously injection of murine 4T1 cells (5×10^6) suspended in 200 μL to the indicated location in BALB/c mice was carried out to obtain the 4T1 subcutaneous xenograft mice. All animals were maintained under aseptic conditions and were housed in a group of five in standard cages with free access to food and water and a 12 h light/dark cycle.

In cells anticancer effect of CSQ-Ph. HeLa, A549 and 4T1 cells were cultured at 37°C in a 5% CO_2/95% air in a 96-well plate at a density of 1×10^4 cells for 24 hours. The solution of **CSQ-Ph** (at the concentrations of 0, 2, 6, 8, and 10 μM) was added to the 96-well plate with/without 808 nm laser (250 mW/cm^2) irradiation for 2, 5 min, respectively. Finally, the cell viability was assessed by standard MTT assay to verify the phototherapy effect.

In vivo PTT effect of CSQ-Ph. After tumor xenografts were established, they were randomly divided into three groups in each xenograft model: PBS group, **CSQ-Ph** (100 μL, 500 μM) inject tumor group and **CSQ-Ph** (100 μL, 500 μM) intravenous injection group. Animals in the PBS group were given the same volume of blank PBS each time. Post-injection, tumors in the irradiation groups were continued exposed to 808 nm laser at the power density of 375 mW/cm^2 for 10 min, the change of temperature was real-time recorded by thermal imager.

In vivo anticancer effect of CSQ-Ph. After tumor xenografts were established, they were randomly divided into five groups in each xenograft model: PBS non-radiation group, PBS irradiation group, **CSQ-Ph** non-radiation group, **CSQ-Ph** (100 μL, 500 uM, IT) irradiation group and **CSQ-Ph** (100 μL, 500 uM, IV) irradiation group. Animals in the PBS non-radiation group and PBS irradiation group were given the same volume of PBS each time. Post-injection, tumors in the irradiation groups were exposed to an 808 nm laser at the power density of 375 mW/cm^2 for 10 min. Tumor volumes and body weights were recorded during the treatments. After treated 14 days, animals were sacrificed, and tumors were dissected and measured.

Hematoxylin and eosin (H&E) histological analysis and blood sample analysis. The major organs from each group were also collected for H&E staining and blood sample analysis to determine the toxicside effect of this treatment. Heart, liver, spleen, lung kidney and tumor of normal mice, tumor-bearing mice for inject tumor group and tumor-bearing mice for intravenous injection group, tissue of each group were excised and fixed in 10% formaldehyde and embedded in paraffin. Then the tissue were prepared to frozen sections and stained with hematoxylin and eosin (H&E) to confirm histology. Commercial assays were used to measure aspartate aminotransferase (AST), alanine aminotransferase (ALT), alkaline phosphatase (ALP), albumin (ALB), UREA, creatinine

(CREA) in blood sample.

2. Compound Synthesis

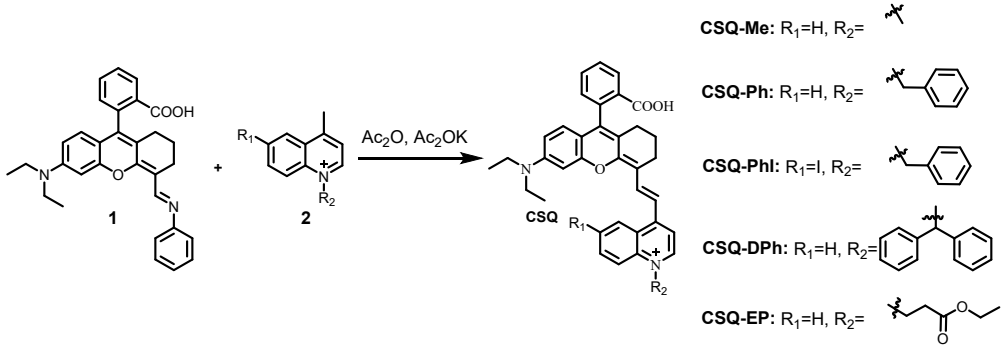

Scheme S1. Preparation of compounds **CSQs**.

Procedure for synthesis of compound 1: Compound **1** was synthesized according to the literature method.

General procedure for synthesis of quinoline salts (compound 2): Quinoline compound (1.0 eq.) and corresponding halohydrocarbon (2.0 eq.) was dissolved in 5 mL CH_3CN under sealed tube at 80 °C for 8 h. Then the reaction was cooled to room temperature, the precipitate was filtered through a Buchner funnel and washed by diethyl ether, the crude product was used to next step without further purified.

General procedure for synthesis of CSQs: Compound **1** (1.0 eq.), potassium acetate (AcOK) and quinoline salt (1.2 eq.) were dissolved in acetic anhydride, and the reaction mixture was heated to 110 °C for 1.5 h. Then, the reaction solution was poured into ice water and perchloric acid was added to precipitate green solids. The precipitate was filtered through a Buchner funnel to give the crude product, which was purified by silica gel flash chromatography eluted with CH_2Cl_2/C_2H_5OH (50:1 to 30:1) to afford compounds **CSQ-Me**, **CSQ-Ph**, **CSQ-PhI**, **CSQ-DPh** and **CSQ-EP** as green solids.

CSQ-Me: Yield, 44.7%. ^{1}H NMR (400 MHz, DMSO-d_6) δ 12.48 (s, 1H), 8.82 (t, *J* = 8.7 Hz, 2H), 8.66 (d, *J* = 14.5 Hz, 1H), 8.26 (d, *J* = 6.9 Hz, 1H), 8.21 (d, *J* = 8.8 Hz, 1H), 8.12 (d, *J* = 7.2 Hz, 1H), 8.07 (dd, *J* = 7.9, 0.9 Hz, 1H), 7.88 – 7.83 (m, 1H), 7.75 (td, *J* = 7.5, 1.2 Hz, 1H), 7.63 (td, *J* = 7.7, 1.0 Hz, 1H), 7.31 – 7.21 (m, 2H), 6.84 (d, *J* = 2.0 Hz, 1H), 6.50 (dd, *J* = 9.0, 2.5 Hz, 1H), 6.38 (d, *J* = 8.9 Hz, 1H), 4.34 (s, 3H), 3.45 (q, *J* = 7.0 Hz, 4H), 2.72 (t, *J* = 5.6 Hz, 2H), 2.18 (ddd, *J* = 21.6, 16.3, 8.8 Hz, 2H), 1.71 (td, *J* = 13.1, 7.1 Hz, 2H), 1.16 (t, *J* = 7.0 Hz, 6H). ^{13}C NMR (100 MHz, DMSO-d_6) δ 172.4, 167.5, 156.8, 154.5, 152.0, 150.1, 145.7, 142.2, 139.2, 138.3, 136.3, 134.4, 132.9, 131.5, 130.9, 130.4, 129.1, 128.3, 126.8, 126.2, 125.7, 120.4, 119.0, 112.9, 112.7, 112.1, 111.8, 109.3, 97.2,

44.3, 43.7, 27.1, 24.7, 21.5, 20.7, 13.0.MS (ESI): calcd for $C_{36}H_{35}N_2O_3^+$ 543.2642, found 543.2642.

CSQ-Ph: Yield, 33.1%. ^{1}H NMR (400 MHz, $CDCl_3$) δ 8.58 (d, *J* = 6.8 Hz, 1H), 8.27 (d, *J* = 14.3 Hz, 1H), 8.17 (d, *J* = 6.8 Hz, 3H), 7.88 (d, *J* = 8.8 Hz, 1H), 7.70 (t, *J* = 7.9 Hz, 1H), 7.61 (t, *J* = 7.6 Hz, 1H), 7.48 (q, *J* = 7.5 Hz, 2H), 7.21 (t, *J* = 7.3 Hz, 2H), 7.13 (d, *J* = 7.7 Hz, 3H), 7.06 (d, *J* = 7.5 Hz, 1H), 6.99 (s, 1H), 6.58 (d, *J* = 14.5 Hz, 1H), 6.47 (d, *J* = 8.8 Hz, 1H), 6.31 (d, *J* = 9.1 Hz, 1H), 5.62 (d, *J* = 15.9 Hz, 1H), 5.14 (d, *J* = 15.9 Hz, 1H), 3.48 (ddd, *J* = 45.7, 15.5, 7.8 Hz, 4H), 2.83 (d, *J* = 19.1 Hz, 1H), 2.31 – 2.15 (m, 1H), 1.97 (s, 2H), 1.85 (s, 1H), 1.39 (s, 1H), 1.21 (t, *J* = 7.9 Hz, 6H). ^{13}C NMR (100 MHz, DMSO-d_6) δ 167.1, 157.4, 154.3, 151.8, 149.9, 144.7, 143.2, 138.6, 138.0, 135.8, 135.2, 130.9, 130.5, 129.9, 129.1, 128.8, 128.4, 127.6, 126.8, 126.6, 126.1, 125.6, 118.7, 113.0, 112.3, 111.9, 111.1, 109.4, 96.6, 57.6, 44.0, 26.6, 24.3, 20.3, 12.6. HRMS: cacld for $[C_{42}H_{39}N_2O_3]^+$ 619.2955, found 619.2955.

CSQ-PhI: Yield, 13.9%. ^{1}H NMR (400 MHz, DMSO-d_6) δ 9.07 (s, 1H), 8.80 (dd, *J* = 7.1, 3.1 Hz, 1H), 8.68 (d, *J* = 13.1 Hz, 1H), 8.17 (q, *J* = 3.7 Hz, 2H), 8.08 (d, *J* = 9.4 Hz, 1H), 7.76 (td, *J* = 9.2, 5.0 Hz, 2H), 7.69 – 7.60 (m, 1H), 7.43 – 7.36 (m, 2H), 7.30 (t, *J* = 4.2 Hz, 2H), 7.18 (dd, *J* = 14.5, 3.1 Hz, 1H), 6.89 (t, *J* = 2.9 Hz, 1H), 6.61 – 6.54 (m, 1H), 6.45 (dd, *J* = 9.0, 3.1 Hz, 1H), 5.92 (s, 2H), 3.47 (t, *J* = 7.4 Hz, 4H), 2.76 (s, 2H), 2.28 – 2.12 (m, 2H), 1.24 (d, *J* = 8.7 Hz, 4H), 1.15 (d, *J* = 7.3 Hz, 6H). MS(ESI): cacld for $[C_{42}H_{38}IN_2O_3]^+$ 745.1922, found 745.1922.

CSQ-DPh: Yield, 27.0%. ^{1}H NMR (400 MHz, $CDCl_3$) δ 8.54 (dd, *J* = 14.2, 4.9 Hz, 1H), 8.39 – 8.29 (m, 1H), 8.20 – 8.10 (m, 1H), 7.82 (dd, *J* = 9.4, 4.5 Hz, 1H), 7.73 (t, *J* = 6.3 Hz, 2H), 7.63 – 7.56 (m, 2H), 7.54 – 7.49 (m, 1H), 7.44 – 7.34 (m, 6H), 7.28 (t, *J* = 6.1 Hz, 2H), 7.14 (t, *J* = 6.5 Hz, 4H), 6.92 (dd, *J* = 14.3, 4.7 Hz, 1H), 6.53 (q, *J* = 7.5 Hz, 2H), 6.40 (q, *J* = 8.3 Hz, 1H), 3.38 (q, *J* = 6.9 Hz, 4H), 3.30 (d, *J* = 5.9 Hz, 1H), 2.65 (q, *J* = 6.2 Hz, 2H), 2.21 (q, *J* = 6.0 Hz, 2H), 1.73 (dt, *J* = 12.2, 5.8 Hz, 2H), 1.15 (d, *J* = 10.4 Hz, 6H). ^{13}C NMR (100 MHz, $CDCl_3$) δ 160.8, 151.2, 139.6, 136.8, 134.1, 132.9, 131.7, 129.9, 129.7, 129.2, 129.1, 129.1, 127.3, 125.7, 110.6, 96.6, 69.7, 45.1, 29.9, 27.1, 25.3, 20.9, 12.8. HRMS: cacld for $[C_{48}H_{43}N_2O_3]^+$ 695.3268, found 695.3267.

CSQ-EP: Yield, 31.4%. ^{1}H NMR (400 MHz, $CDCl_3$) δ 8.62 – 8.47 (m, 1H), 8.32 – 8.15 (m, 2H), 8.09 – 7.89 (m, 3H), 7.83 (s, 1H), 7.64 (s, 2H), 7.55 (d, *J* = 8.6 Hz, 1H), 7.11 (d, *J* = 7.5 Hz, 1H), 6.91 (s, 1H), 6.57 – 6.32 (m, 3H), 4.81 (s, 1H), 4.32 (s, 1H), 4.05 (s, 2H), 3.53 (d, *J* = 25.8 Hz, 4H), 2.88 (s, 2H), 2.23 (d, *J* = 14.9 Hz, 1H), 2.05 (s, 2H), 1.74 (s, 1H), 1.41 (s, 2H), 1.27 (s, 6H), 1.15 (s, 3H). ^{13}C NMR (100 MHz, $CDCl_3$) δ 170.6, 168.4, 157.6, 154.9, 151.6, 143.6, 143.1, 137.8, 137.7, 137.0, 134.1, 133.1, 131.5, 130.1, 129.6, 129.2, 128.7, 128.0, 127.4, 126.8, 125.7, 125.2, 117.6, 114.3, 112.2, 111.5, 102.7, 97.2, 91.9, 60.6, 50.2, 45.1, 33.0, 26.4, 23.7, 19.9, 17.7, 14.0, 12.7, 1.0. HRMS: cacld for $[C_{40}H_{41}N_2O_5]^+$ 629.3010, found 629.3008.

3. Supplemental Table and Figures

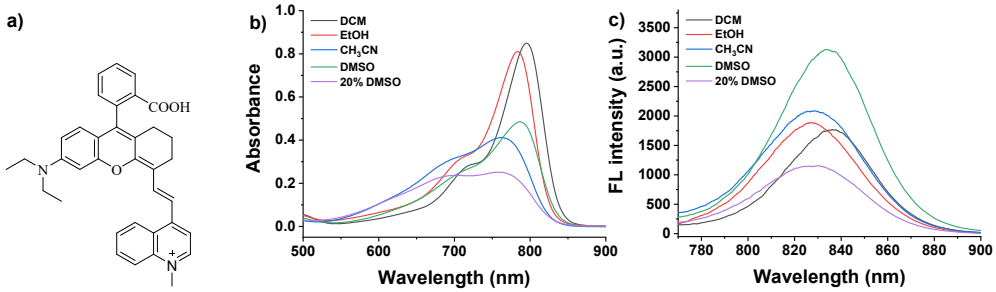

Solvent	ε(M^{-1}*c m^{-1})	λ_{abs} (nm)	λ_{em}(nm)	Stokes Shift(nm)	Φ_f
DCM	84900	796	836	40	1.70%
EtOH	81000	784	827	43	2.08%
CH_3CN	41200	763	828	65	1.54%
DMSO	48500	787	834	47	4.58%
PBS(20%DMSO)	75800	758	829	71	0.88%

Figure S1. a) Chemical structure of **CSQ-Me**. b) Absorption and c) emission spectra of **CSQ-Me** (10 μM) in different solvents, λ_{ex} = 760 nm.

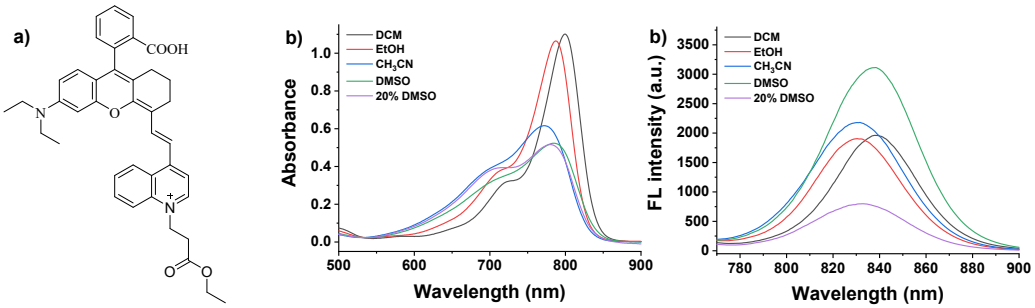

Solvent	ε(M^{-1}*c m^{-1})	λ_{abs} (nm)	λ_{em}(nm)	Stokes Shift(nm)	Φ_f
DCM	110100	800	839	39	3.02%
EtOH	106500	787	830	43	3.76%
CH_3CN	61600	773	831	58	1.12 %
DMSO	52300	786	838	52	5.56 %
PBS(20%DMSO)	51600	780	833	33	1.45%

Figure S2. a) Chemical structure of **CSQ-EP**. b) Absorption and c) emission spectra of **CSQ-EP** (10 μM) in different solvents, λ_{ex} = 760 nm.

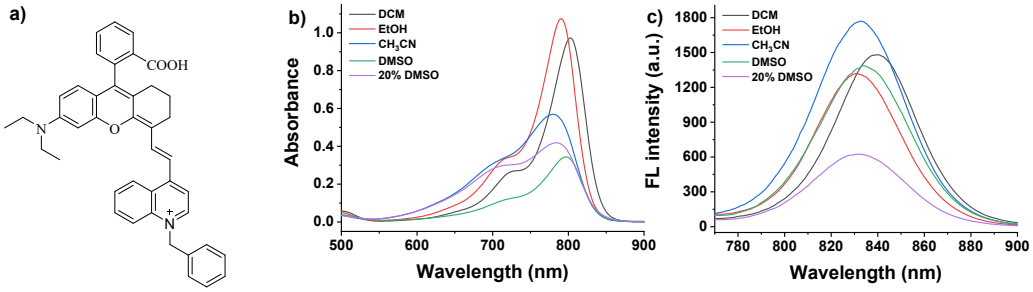

Solvent	ε(M^{-1}*c m^{-1})	λ_{abs} (nm)	λ_{em}(nm)	Stokes Shift(nm)	Φ_f
DCM	97300	803	839	36	2.80%
EtOH	107400	790	830	40	2.60%
CH_3CN	56900	782	833	51	0.83%
DMSO	34400	797	833	36	3.29%
PBS(20%DMSO)	41900	784	830	46	1.37%

Figure S3. a) Chemical structure of **CSQ-Ph**. b) Absorption and c) emission spectra of **CSQ-Ph** (10 μM) in different solvents, λ_{ex} = 760 nm.

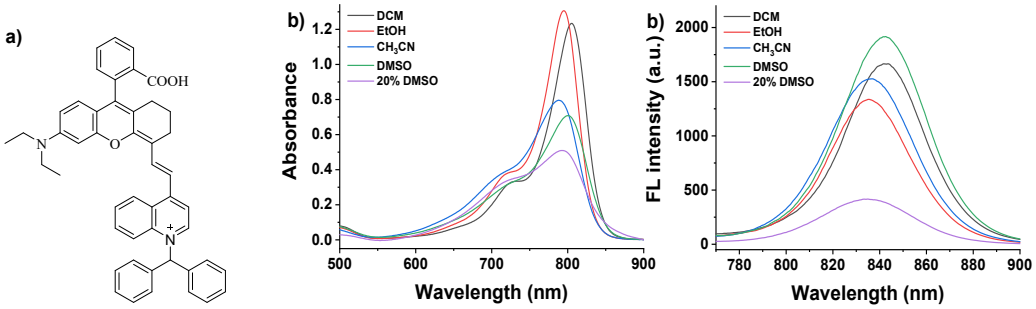

Solvent	ε(M^{-1}*cm^{-1})	λ_{abs} (nm)	λ_{em}(nm)	Stokes Shift(nm)	Φ_f
DCM	123400	805	843	38	2.94 %
EtOH	130600	795	835	40	2.26 %
CH_3CN	79600	788	836	48	0.96%
DMSO	70800	800	842	42	2.86%
PBS(20%DMSO)	50900	793	834	41	0.87%

Figure S4. a) Chemical structure of **CSQ-DPh**. b) Absorption and c) emission spectra of **CSQ-DPh** (10 μM) in different solvents, λ_{ex} = 760 nm.

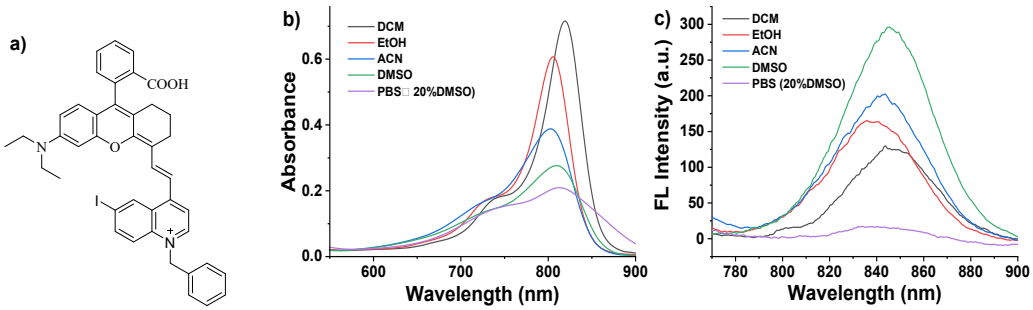

Solvents	ε(M^{-1}* cm^{-1})	λ_{abs} (nm)	λ_{em}(nm)	Stokes Shift(nm)
DCM	71581	819	844	25
EtOH	60677	806	840	34
ACN	38805	803	843	40
DMSO	27634	809	845	36
PBS (20% DMSO)	20918	803	837	34

Figure S5. a) Chemical structure of **CSQ-PhI**. b) Absorption and c) emission spectra of **CSQ-PhI** (10 μM) in different solvents, λ_{ex} = 760 nm.

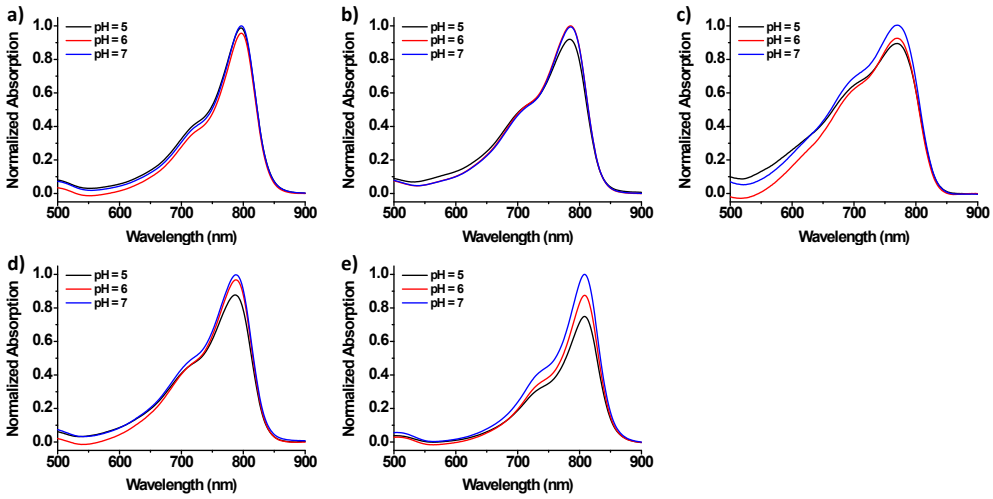

Figure S6. Normalized absorption spectra of a) **CSQ-DPh**, b) **CSQ-EP**, c) **CSQ-Me**, d) **CSQ-Ph**, e) **CSQ-PhI** were measured in at different pH (5-7) value solution.

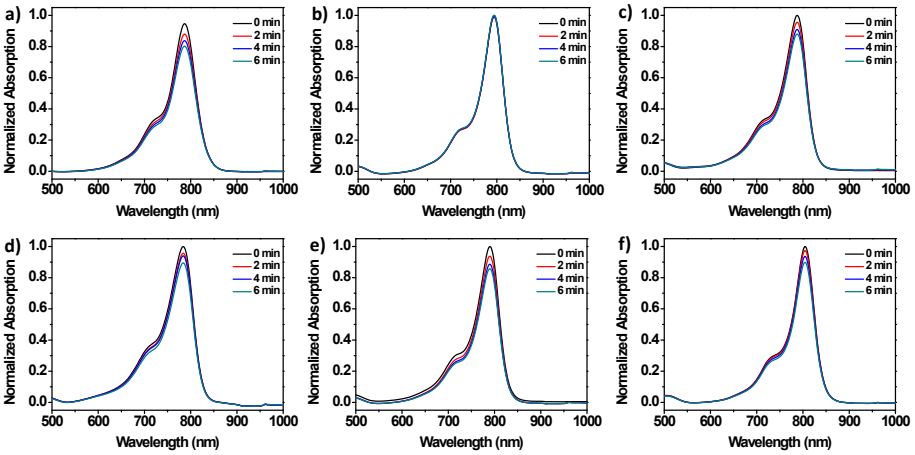

Figure S7. Photostability assay of a) ICG, b) **CSQ-DPh**, c) **CSQ-EP**, d) **CSQ-Me**, e) **CSQ-P**h, f) **CSQ-PhI** were measured in EtOH solution with the same power density laser (808 nm).

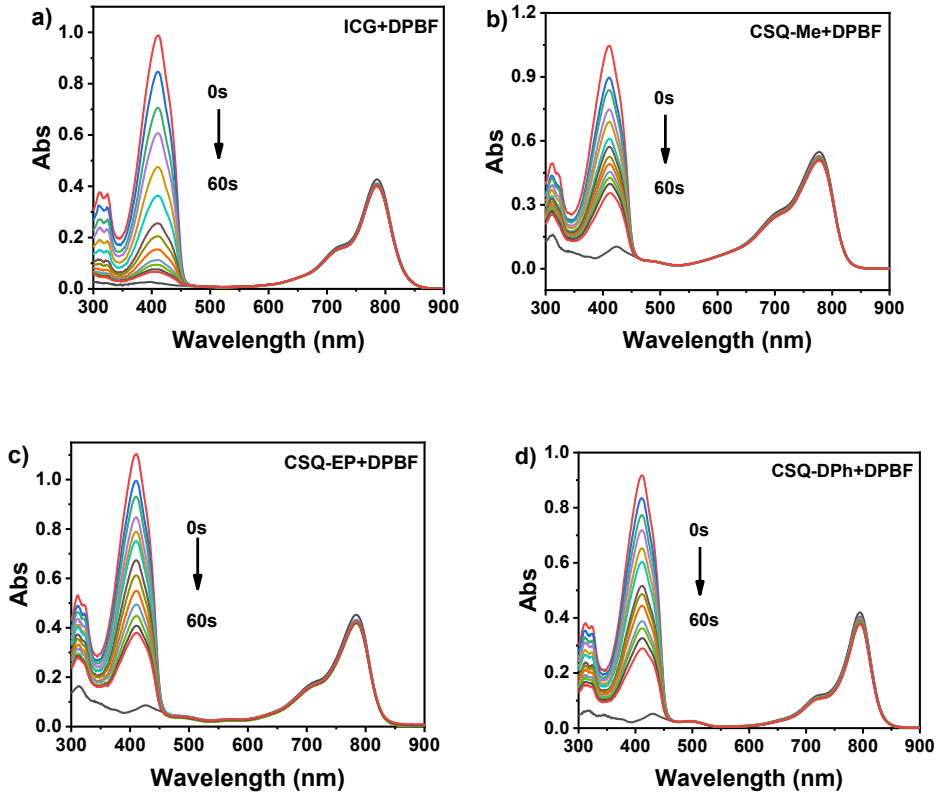

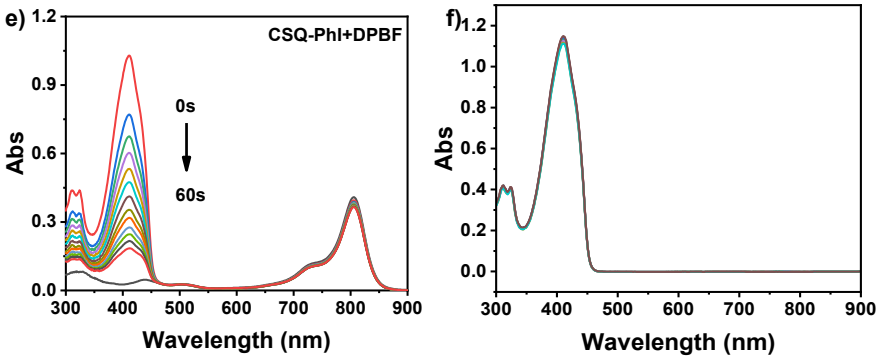

Figure S8. Time-dependent photodegradation of DPBF (50 μM) in the presence of **CSQs** (a) **ICG**, b) **CSQ-Me**, c) **CSQ-EP**, d) **CSQ-DPh**, e) **CSQ-PhI**.) or in the absence of **CSQs** (f) upon 808 nm laser (250 mW/cm^2) irradiation in methanol solution.

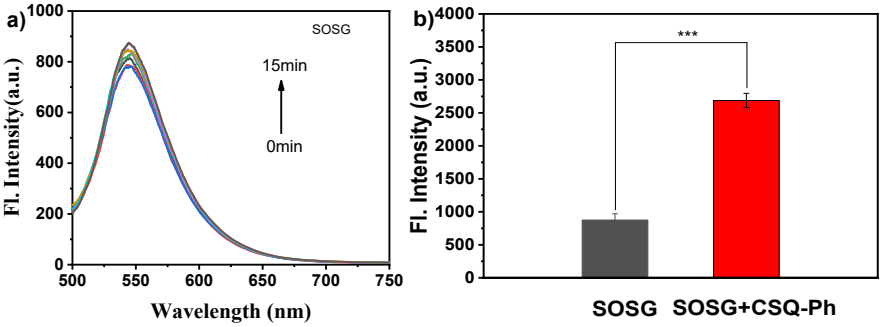

Figure S9. Time-dependent photodegradation of SOSG (10 μM) in the absence of **CSQ-Ph** (5 μM) upon 808 nm laser (250 mW/cm^2) irradiation in methanol solution, b) The photodegradation intensity of SOSG (10 μM) in the absence or presence of **CSQ-Ph** (5 μM) upon 808 nm laser (250 mW/cm^2) irradiation in methanol solution, the fluorescence signal of indicator was monitored in a range of 500-750 nm with a 480 nm excitation; Error bar = relative standard deviation (RSD; n = 3, *p < 0.05, **p < 0.01, ***p < 0.001).

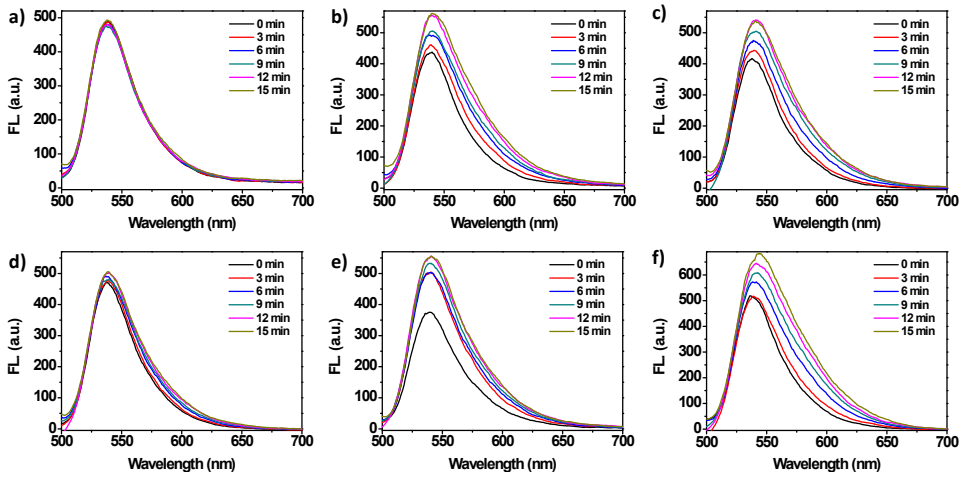

Figure S10. DHR123 probe sensing $O_2^{\bullet-}$ production in EtOH solution a) blank b) **CSQ-DPh** c) **CSQ-EP** d) **CSQ-Me** e) **CSQ-Ph** f) **CSQ-PhI**, Ex: 480 nm, Em: 500-700 nm.

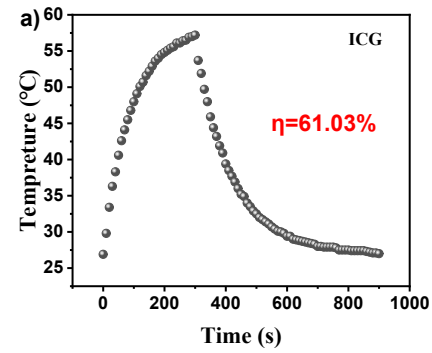
a)
ICG
η=61.03%
Tempreture (℃)
Time (s)

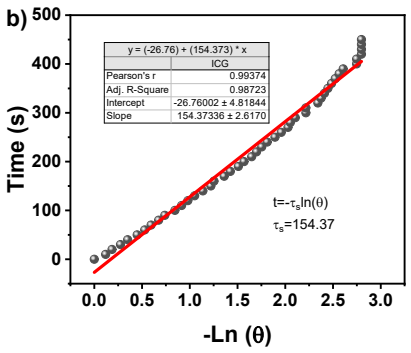
b)
y = (-26.76) + (154.373) * x
ICG
Pearson's r 0.99374
Adj. R-Square 0.98723
Intercept -26.76002 ± 4.81844
Slope 154.37336 ± 2.6170
t=-τs ln(θ)
τs=154.37
Time (s)
-Ln (θ)

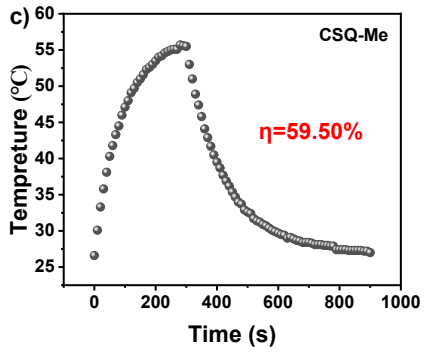
c)
CSQ-Me
η=59.50%
Tempreture (℃)
Time (s)

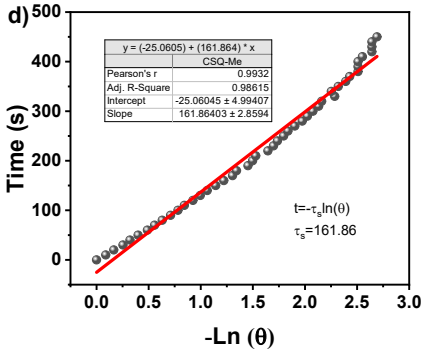
d)
y = (-25.0605) + (161.864) * x
CSQ-Me
Pearson's r 0.9932
Adj. R-Square 0.98615
Intercept -25.06045 ± 4.99407
Slope 161.86403 ± 2.8594
t=-τs ln(θ)
τs=161.86
Time (s)
-Ln (θ)

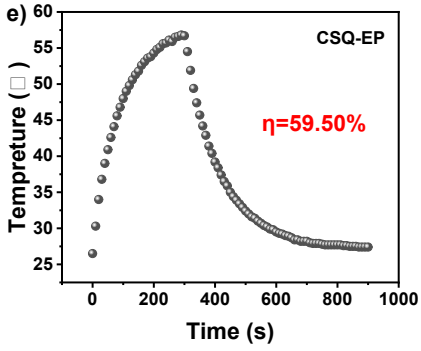
e)
CSQ-EP
η=59.50%
Tempreture ( )
Time (s)

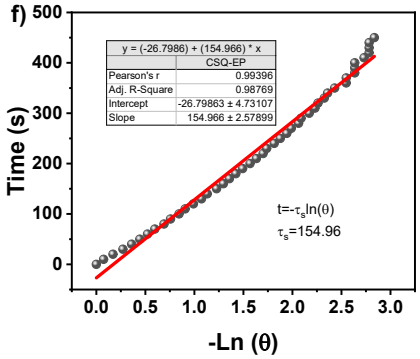
f)
y = (-26.7986) + (154.966) * x
CSQ-EP
Pearson's r 0.99396
Adj. R-Square 0.98769
Intercept -26.79863 ± 4.73107
Slope 154.966 ± 2.57899
t=-τs ln(θ)
τs=154.96
Time (s)
-Ln (θ)

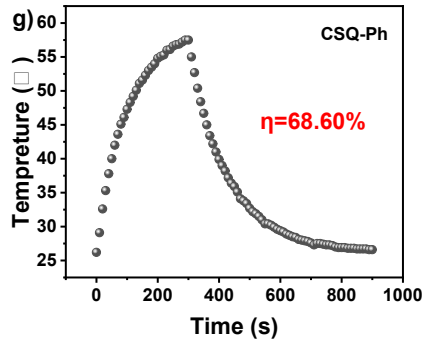
g)
CSQ-Ph
η=68.60%
Tempreture ( )
Time (s)

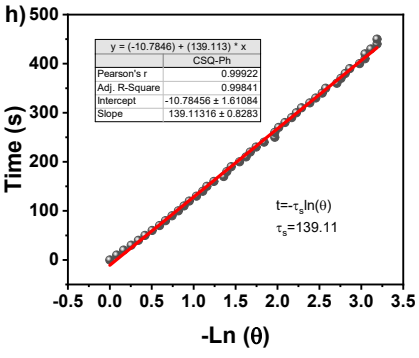
h)
y = (-10.7846) + (139.113) * x
CSQ-Ph
Pearson's r 0.99922
Adj. R-Square 0.99841
Intercept -10.78456 ± 1.61084
Slope 139.11316 ± 0.8283
t=-τs ln(θ)
τs=139.11
Time (s)
-Ln (θ)

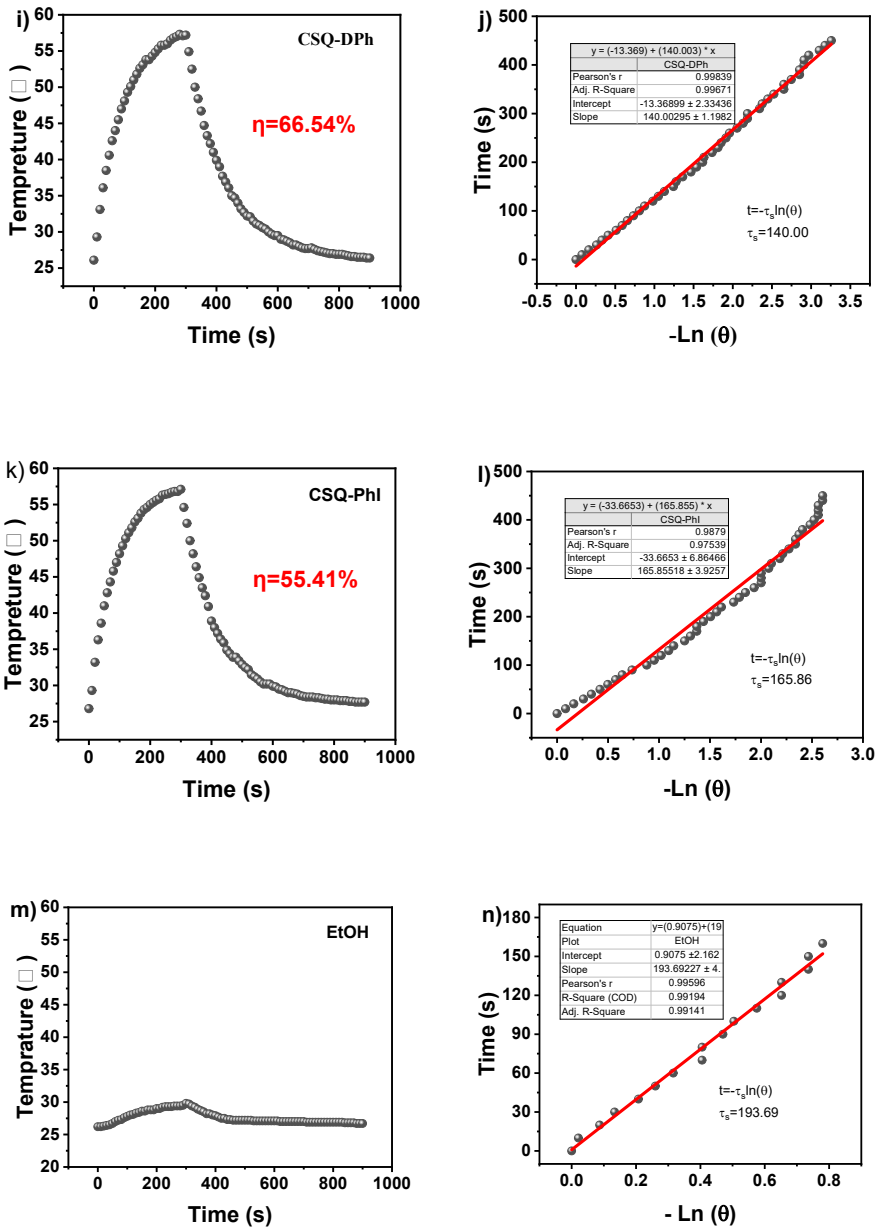

Figure S11. Photothermal performance of a) **ICG**, c) **CSQ-Me**, e) **CSQ-EP**, g) **CSQ-Ph**, i) **CSQ-DPh**, k) **CSQ-PhI** and ethanol (m) under 808 nm laser (250 mW/cm^2) irradiation for heating and cooling period; Linear time data (b) **ICG**, d) **CSQ-Me**, f) **CSQ-Ep**, h) **CSQ-Ph**, j) **CSQ-DPh**, l) **CSQ-PhI**, n) ethanol) versus –Ln(θ) obtained from the cooling period.

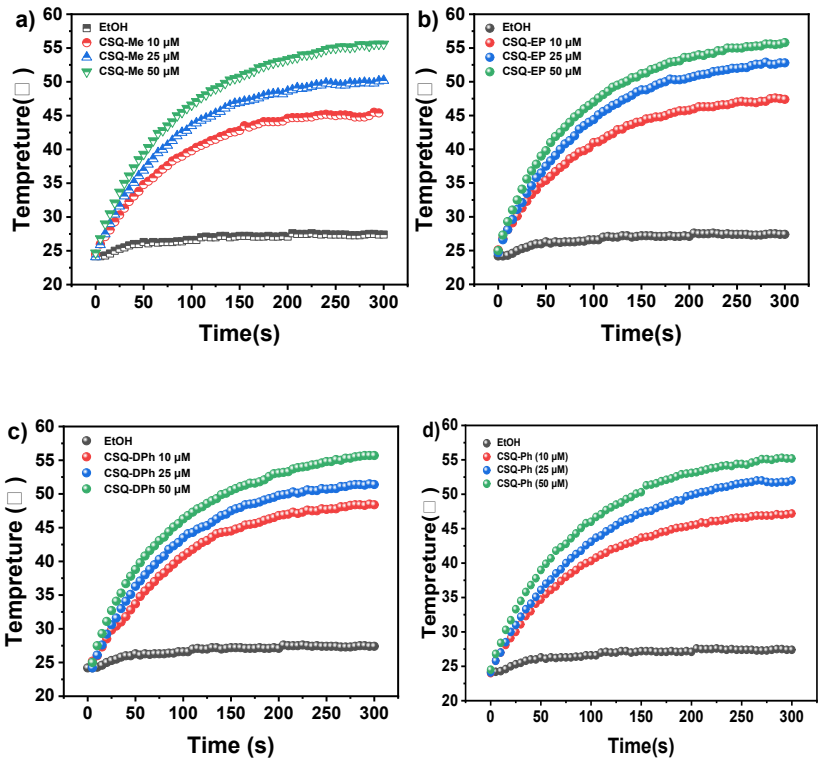

Figure S12. Photothermal features of **CSQs** at various concentrations under 808 nm (250 mW/cm^2) laser irradiation for 5 min in ethanol solution; a) **CSQ-Me**, b) **CSQ-EP**, c) **CSQ-DPh**, d) **CSQ-DPh**.

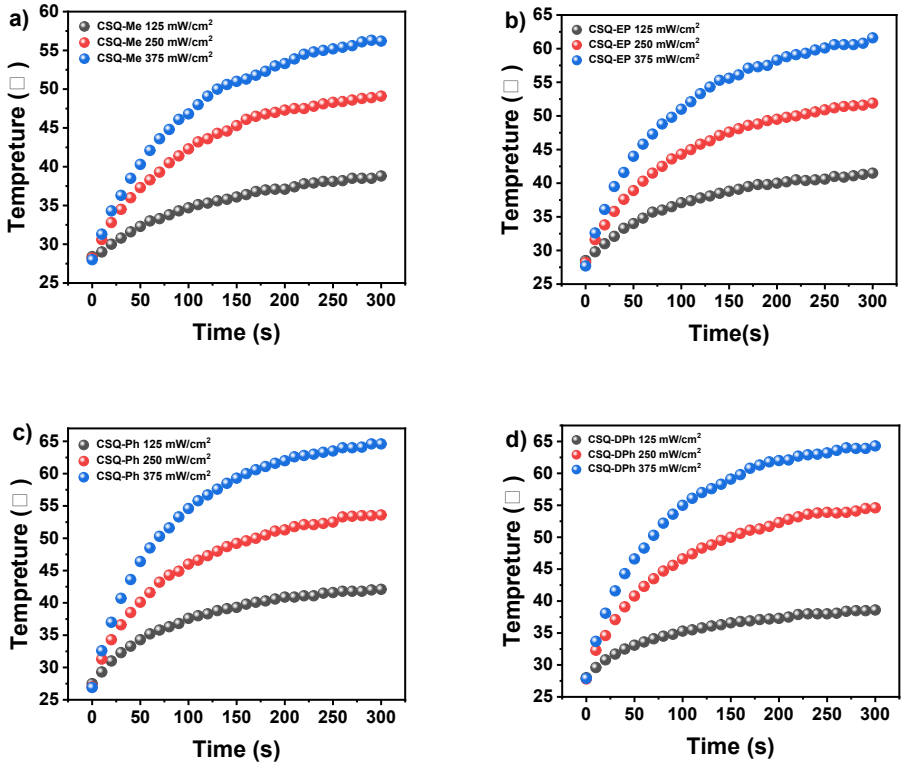

Figure S13. Photothermal features of **CSQs** (50 μM) at various power density under 808 nm laser irradiation for 5 min in ethanol solution; a) **CSQ-Me**, b) **CSQ-EP**, c) **CSQ-Ph**, d) **CSQ-DPh**.

Table S1. The corresponding properties of **CS** and **CSQs**.

Compounds	λ_{abs}	Φ_f	ΔE_{st}
CS	701 nm	41.0%	0.66ev
CSQ-Me	784 nm	2.08%	0.65ev
CSQ-EP	787 nm	3.76%	0.66ev
CSQ-Ph	790 nm	2.60%	0.65ev
CSQ-DPh	795 nm	2.26%	0.65ev

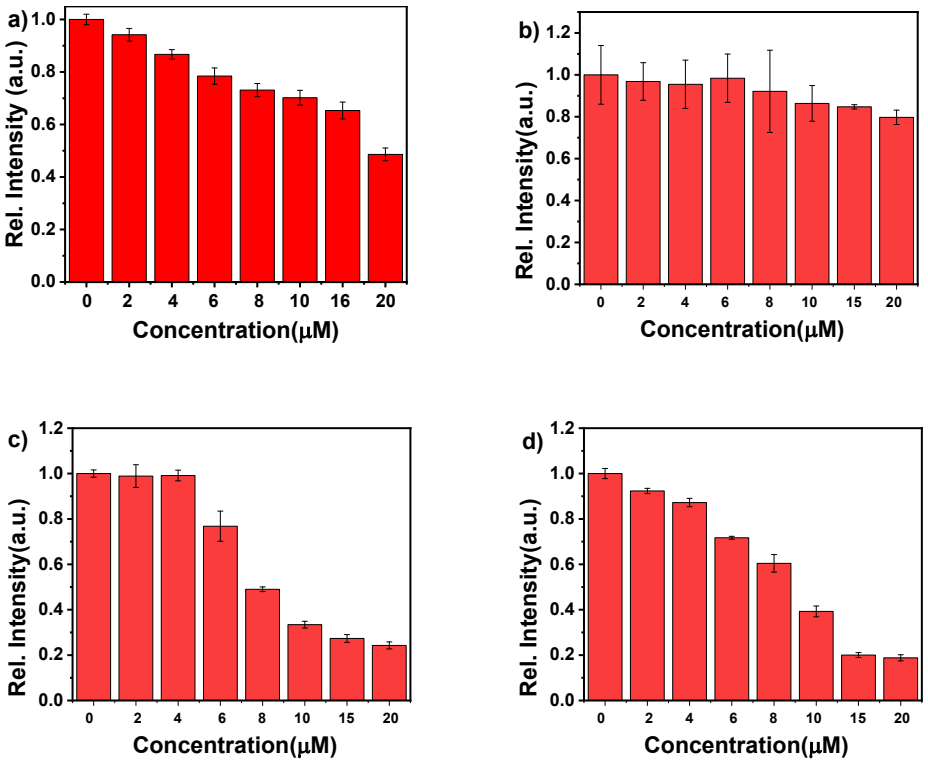

Figure S14. MTT assay for estimating cell viability (%) of HeLa cells incubated with **CSQs** dye at corresponding concentration for 24 h; a) **CSQ-Me**, b) **CSQ-EP**, c) **CSQ-DPh**, d) **CSQ-PhI**. Error bars represent the standard deviations of 3 trials.

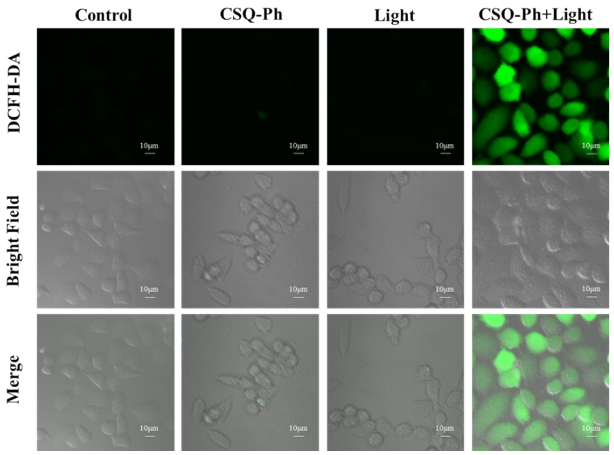

Figure S15. Reactive oxygen species (ROS) detection in HeLa cells under different conditions using DCFH-DA (5 μM, λ_{ex} = 488 nm, λ_{em} = 500~550 nm) as the fluorescence indicator; Control group, **CSQ-Ph** (5 μM) group, light irradiation group, **CSQ-Ph** (5 μM) + light irradiation group; The light irradiation was carried out with 808 nm laser at the power density of 375 mW/cm^2 for 1 min after the addition of **CSQ-Ph** for incubation 30 min, scale bar 10 μm.

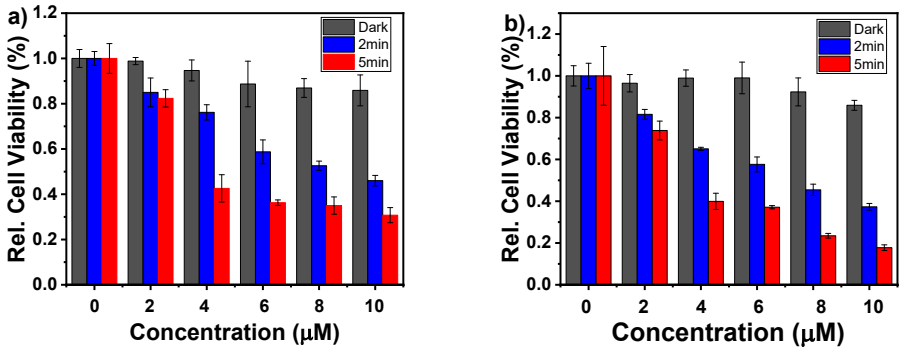

Figure S16. Cell viability of a) A549 and b) 4T1 cells against with **CSQ-Ph** dose under 808 nm (250 mW/cm^2) laser non-radiation/irradiation for different time; Error bars represent the standard deviations of 3 trials.

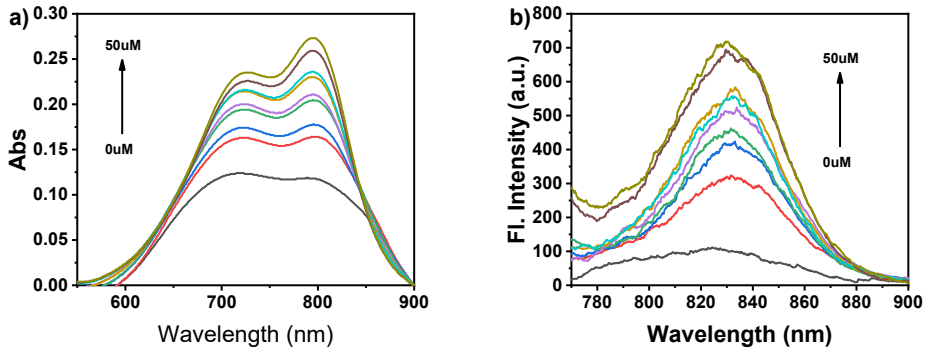

Figure S17. a) Absorption and b) emission spectra of mixed solution of **CSQ-Ph** (10 μM) with different concentration of BSA in PBS solution; λ_{ex} = 750 nm.

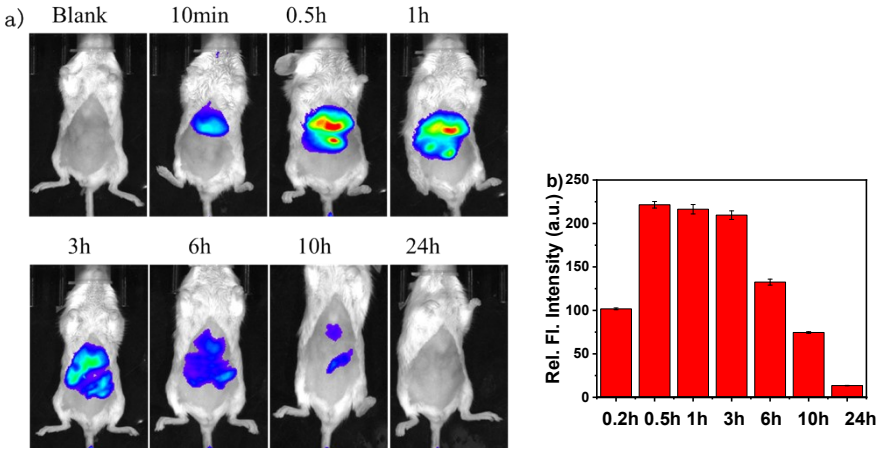

Figure S18. a) Fluorecence imaging of mice at the specific time points after intravenous injection of **CSQ-Ph** (500 μM, 100 μL); b) Relative fluorescence intensity of **CSQ-Ph** at the specific time points; Error bars represent the standard deviations of 3 trials.

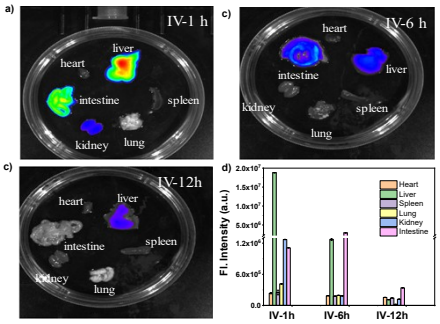

Figure S19. a-c) Fluorescence imaging and d) fluorescence intensities of different organs after different time (a) 1 h, b) 6 h, c) 12 h) the administration of **CSQ-Ph** (500 μM, 100 μL); λ_{ex} = 745 nm, λ_{em} = ICG channel; Error bars represent the standard deviations of 3 trials.

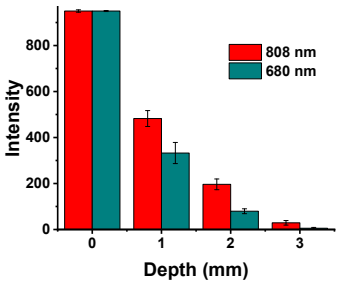

Figure S20. The intensity attenuation of 680 and 808 nm laser in 1% intralipid solution with different thicknesses.

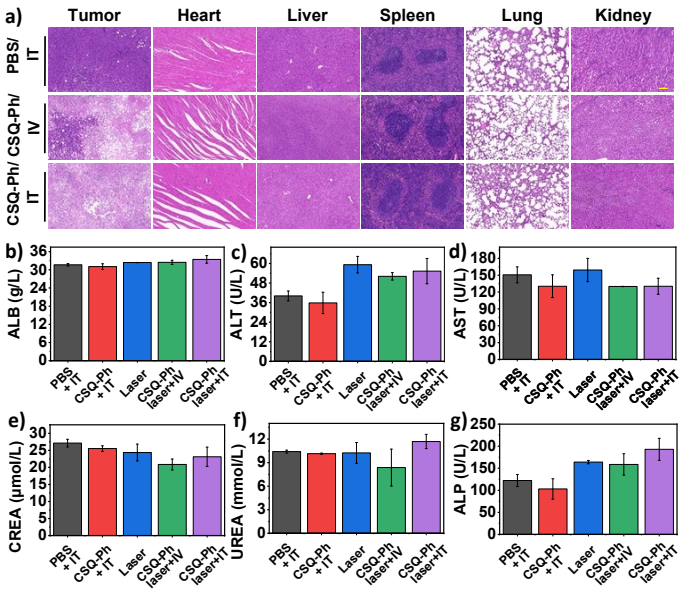

Figure S21. a) H&E-stained tumor, heart, liver, spleen, lung, and kidney slices from mice 24 h post different treatments of euthanized mice, scale bar: 100 μm. Blood biochemical assays using ELISA kits for assessing the levels of (b) ALB, (c) ALT, (d) AST, (e) CREA, (f) UREA, (g) ALP from different groups. Error bar = relative standard deviation (RSD; n = 3)

4. NMR and Mass Spectra

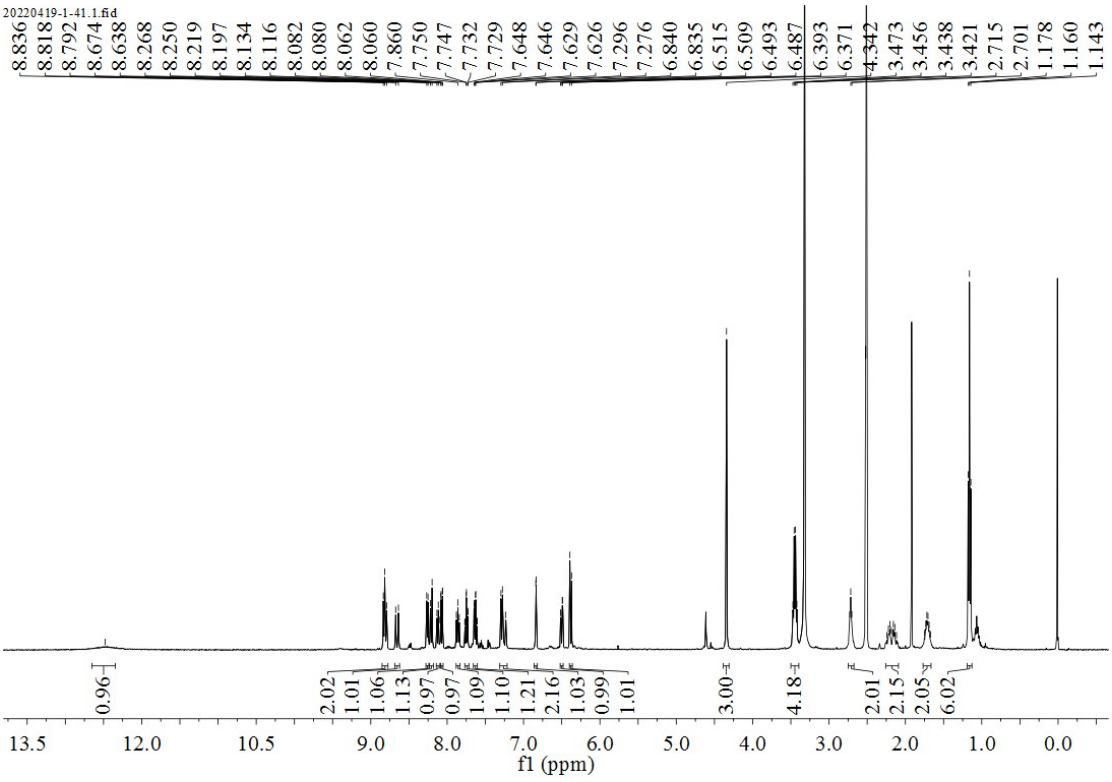

Figure S20. The ^{1}H-NMR spectrum of **CSQ-Me**.

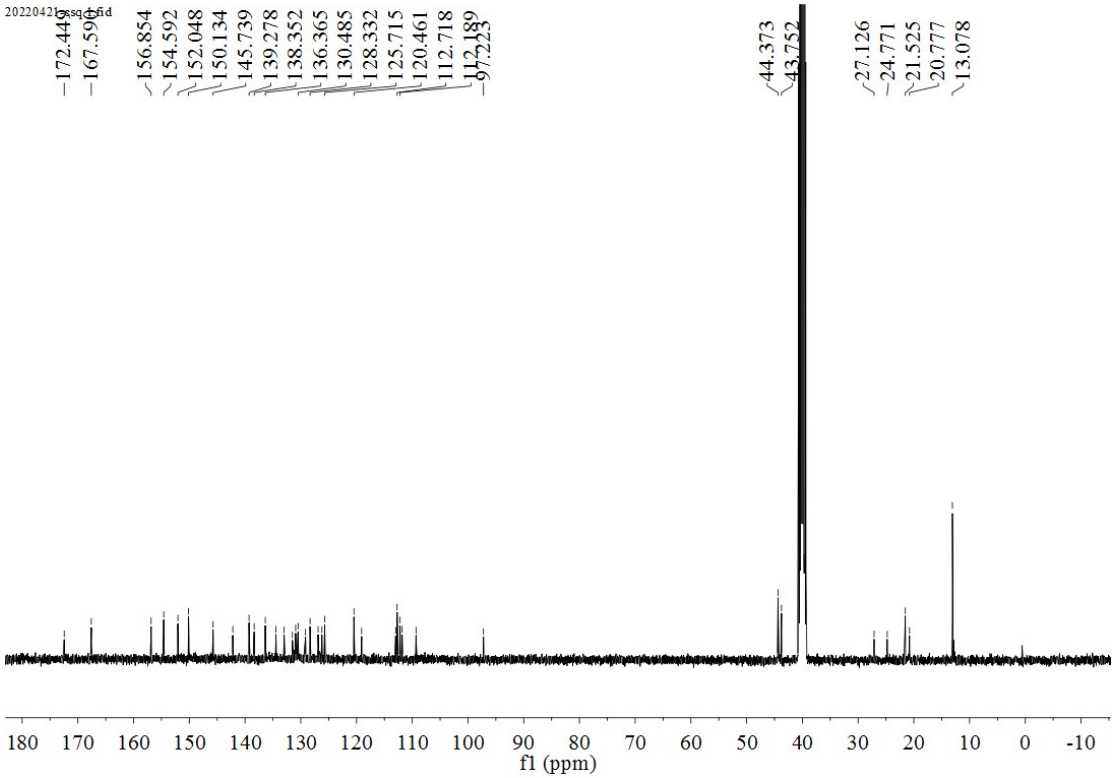

Figure S21. The ^{13}C-NMR spectrum of **CSQ-Me**.

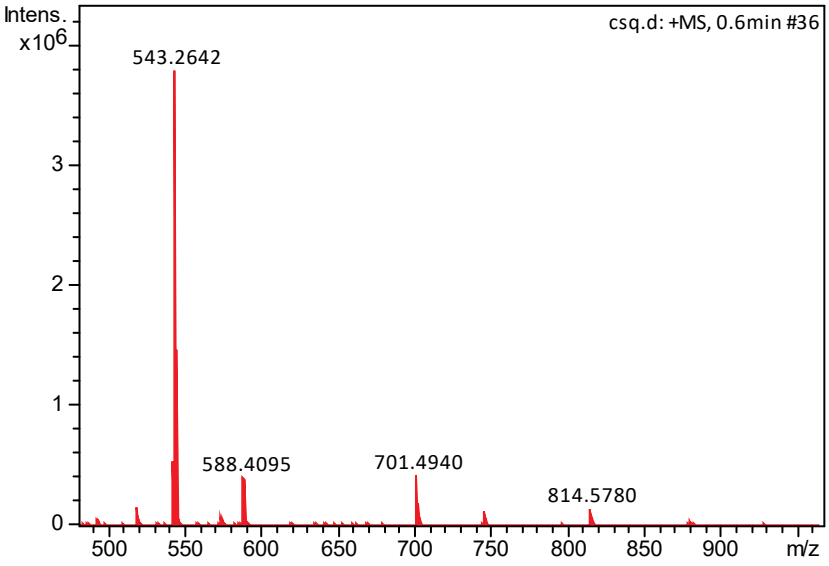

Figure S22. HRMS of **CSQ-Me**.

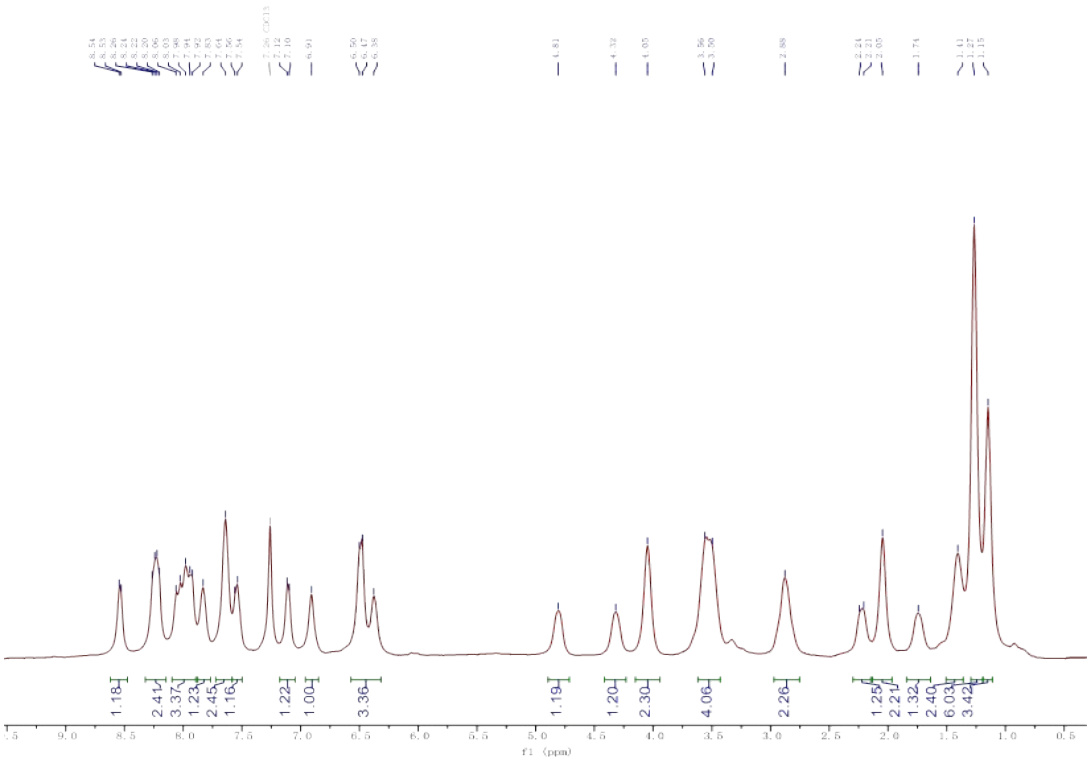

Figure S23. The ^{1}H-NMR spectrum of **CSQ-EP**.

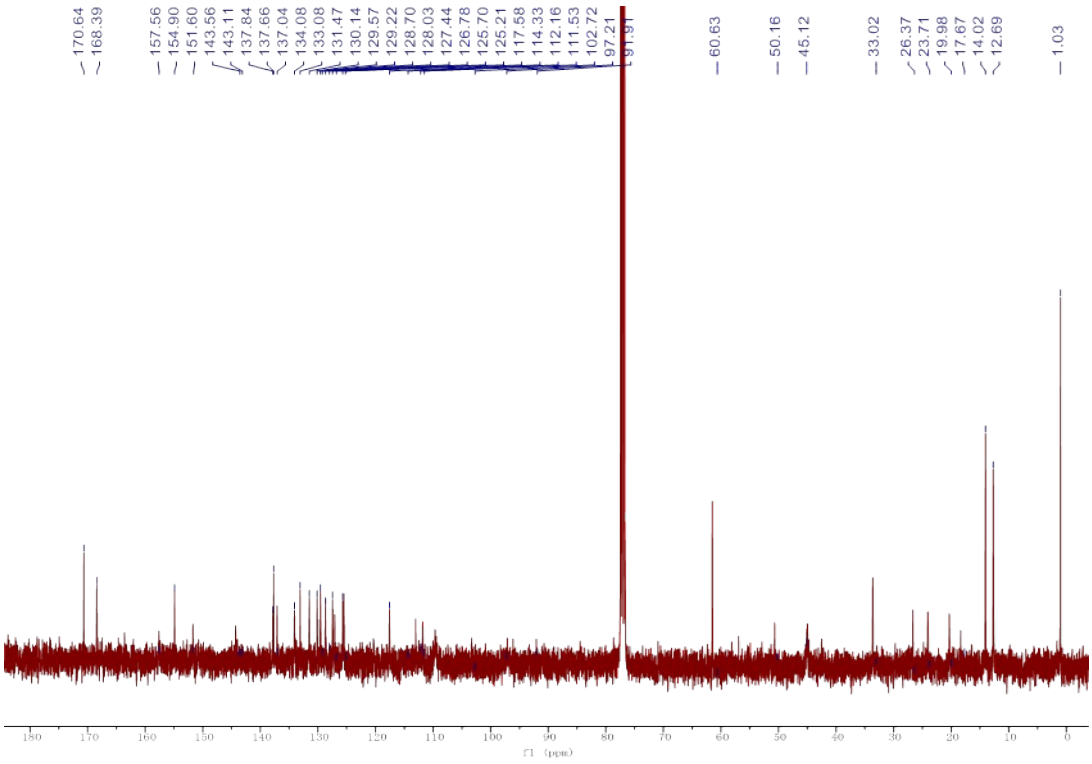

Figure S24. The ^{13}C-NMR spectrum of **CSQ-EP**.

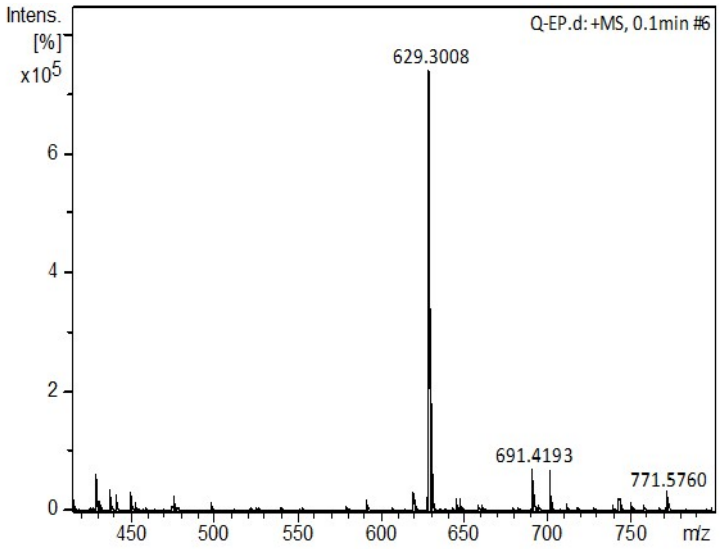

Figure S25. HRMS of **CSQ-EP**.

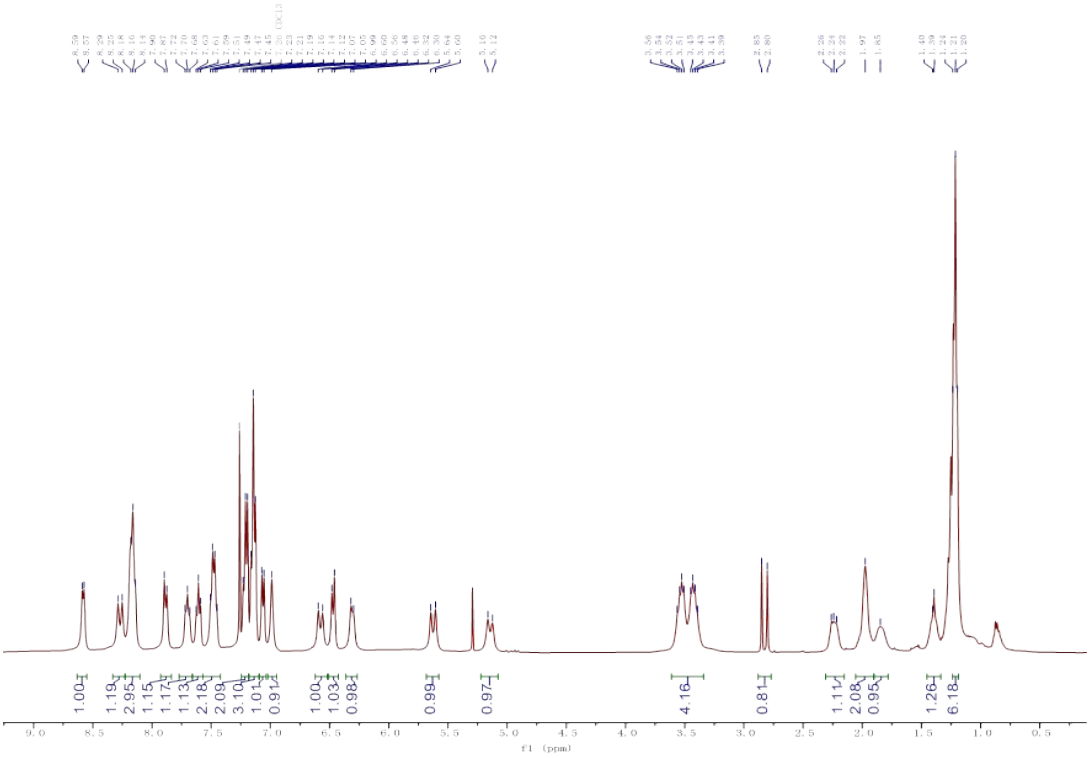

Figure S26. The ^{1}H-NMR spectrum of **CSQ-Ph**.

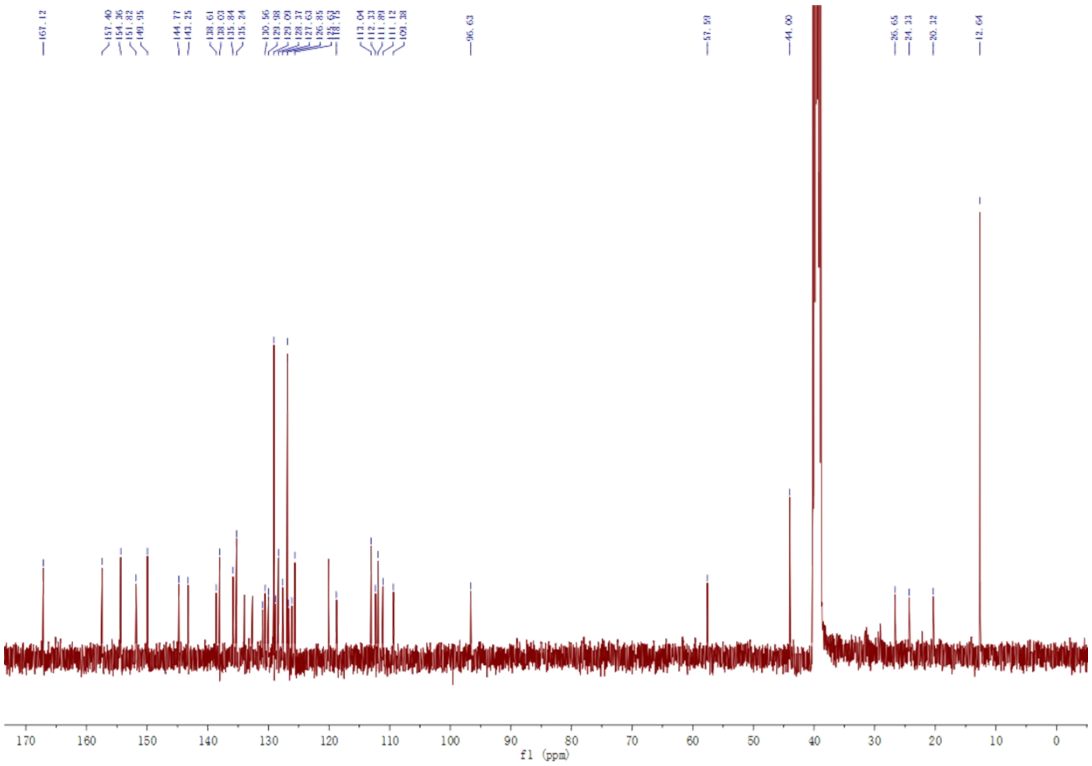

Figure S27. The ^{13}C-NMR spectrum of **CSQ-Ph**.

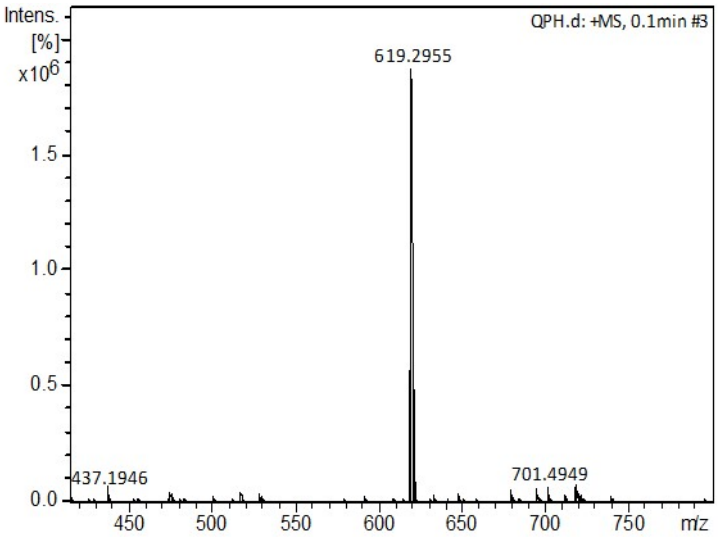

Figure S28. HRMS of **CSQ-Ph**.

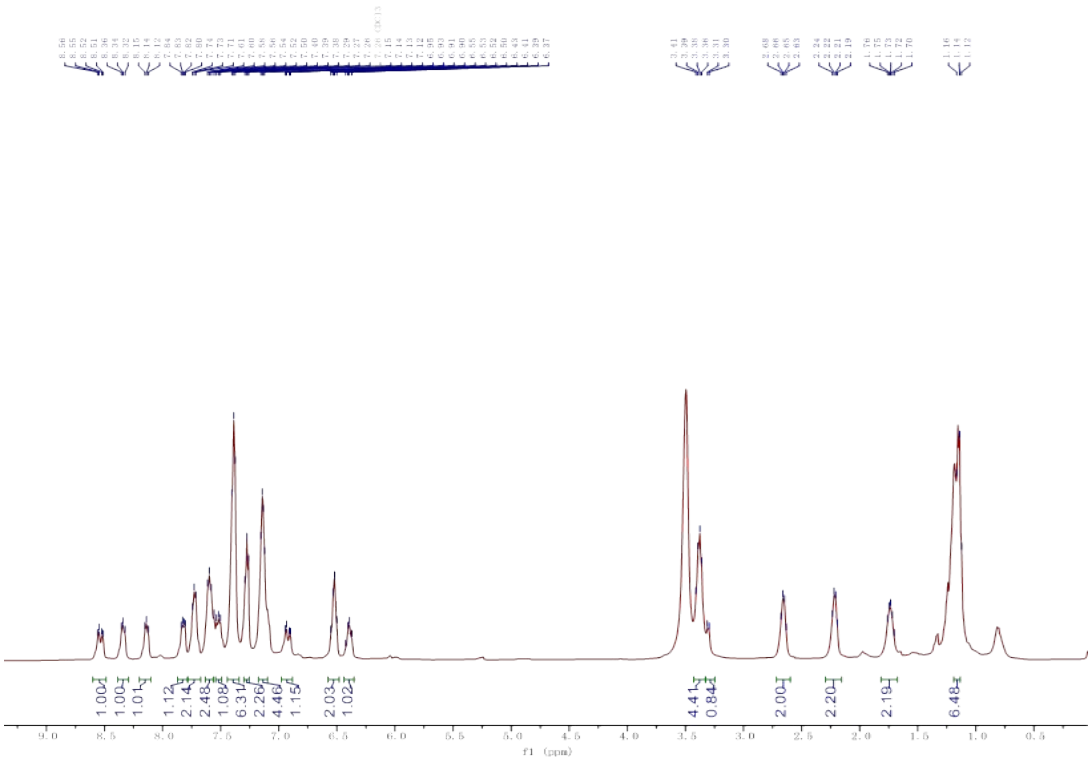

Figure S29. The ^{1}H-NMR spectrum of **CSQ-DPh**.

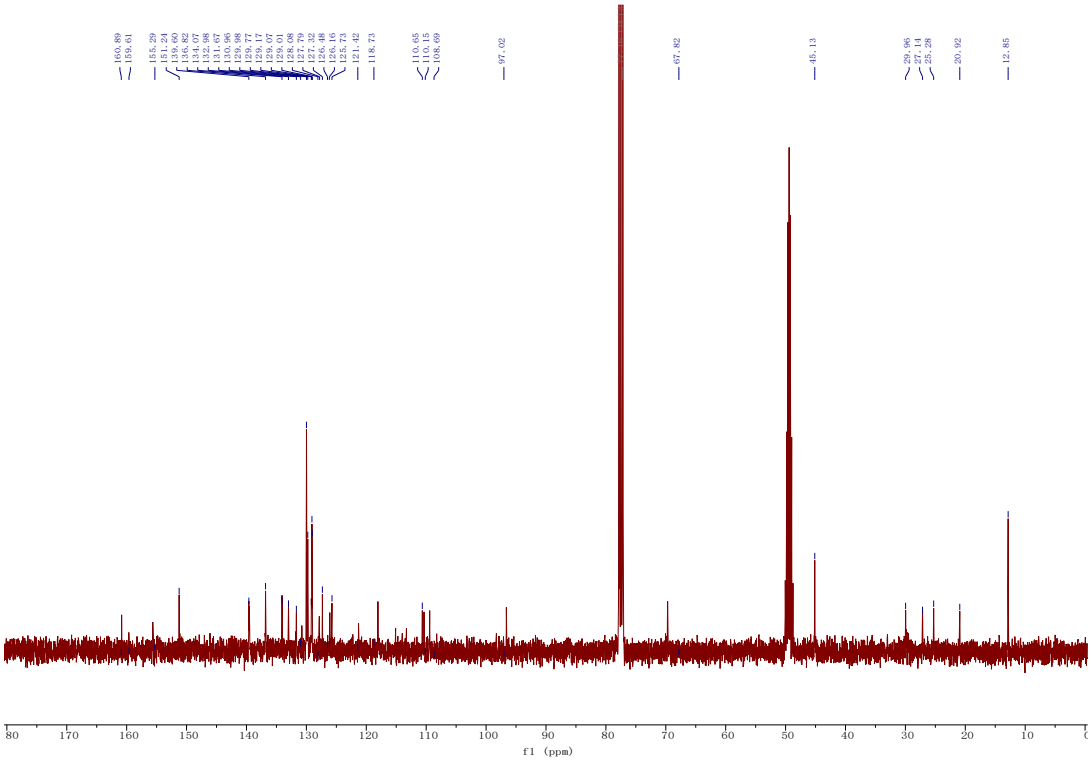

Figure S30. The ^{13}C-NMR spectrum of **CSQ-DPh**.

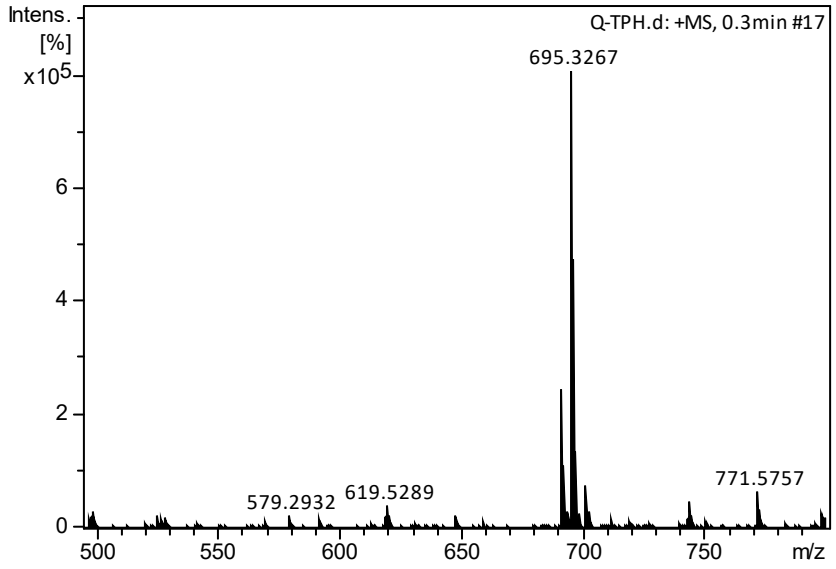

Figure S31. HRMS of **CSQ-DPh**.

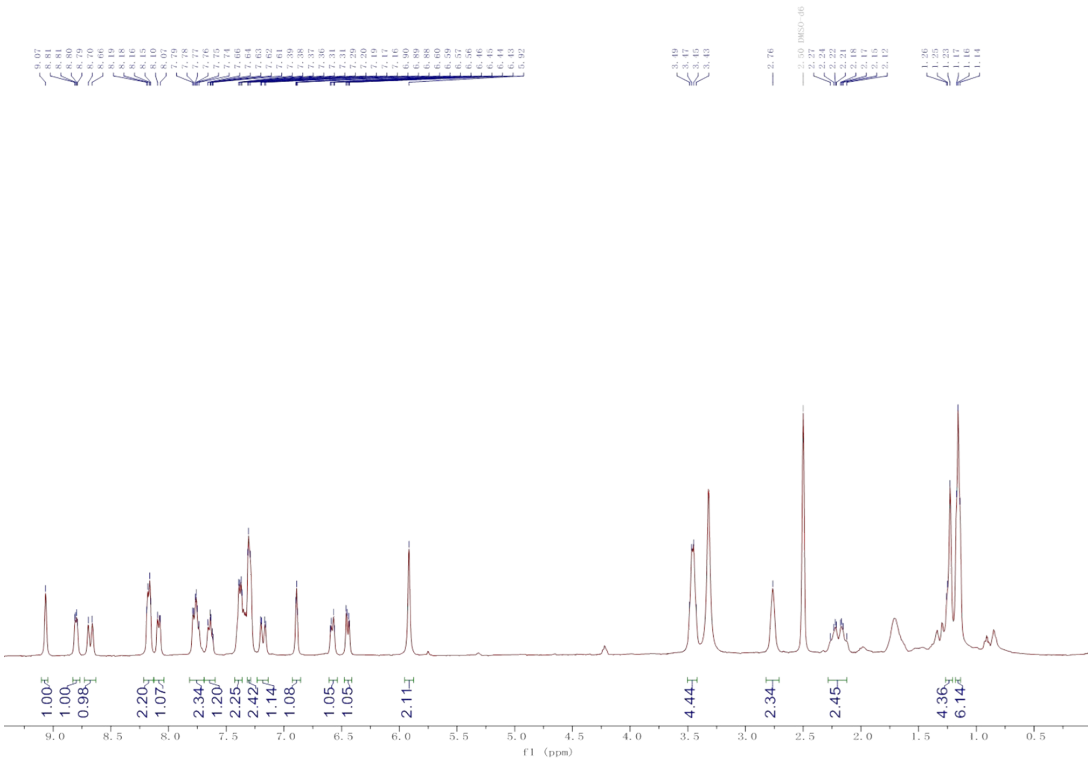

Figure S32. The ^{1}H-NMR spectrum of **CSQ-PhI**.

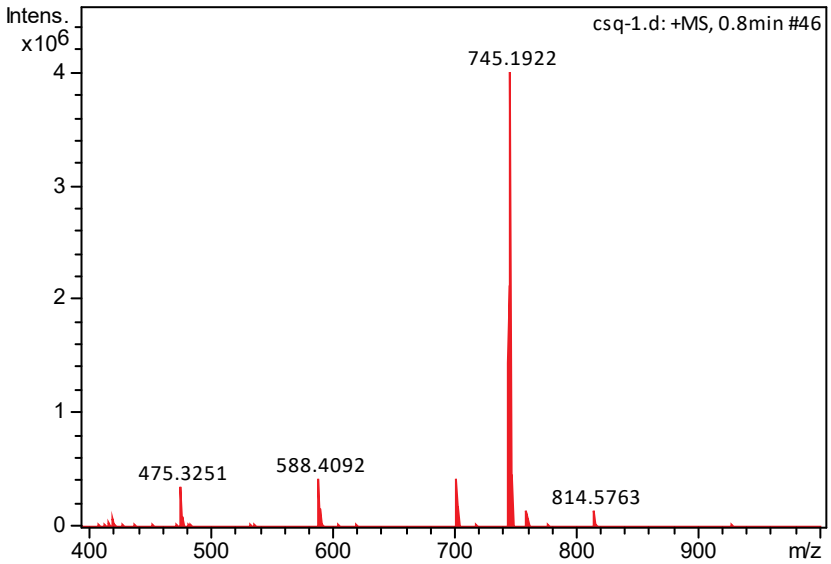

Figure S34. HRMS of **CSQ-PhI**.

5. References

[1] K. Rurack, M. Spieles, *Anal. Chem.* **2011**, *83*, 1232-1242.

[2] M. J. Frisch, G. W. Trucks, H. B. Schlegel, G. E.Scuseria, M. A. Robb, J. R. Cheeseman, G. Scalmani, V. Barone, B. Mennucci, G. A. P. e. al., *Gaussian 09, Revision A.1; Gaussian, Inc.: Wallingford, CT,* **2009**.

[3] S. Reindl, A. Penzkofer, S.-H. Gong, M. Landthaler, R.M. Szeimies, C. Abels, W. B~iumler, *J. Photoch. Photobio. A* **1997**, *105*, 65-68.

[4] X. Z. Zhao, S. R. Long, M. L. Li, J. F. Cao, Y. C. Li, L. Y. Guo, W. Sun, J. J. Du, J. L. Fan, X. J. Peng, *J. Am. Chem. Soc.* **2019**, *142*, 1510-1517.